JOURNAL OF Materials CHEMISTRY

Characterization of the Fermi surface of $(BEDO\text{-}TTF)_5[CsHg(SCN)_4]_2$ by magnetoresistance measurements and tight-binding band structure calculations

Rustem B. Lyubovskii,*[a,d,e] Serguei I. Pesotskii,[a,d,e] Marc Gener,[b] Roger Rousseau,[c] Enric Canadell,*[b] Jos A. A. J. Perenboom,[d] Victor I. Nizhankovskii,[e] Elena I. Zhilyaeva,[a] Olga A. Bogdanova[a] and Rimma N. Lyubovskaya[a]

[a]*Institute of Problems of Chemical Physics, Russian Academy of Sciences, 142432 Chernogolovka, MD, Russia. E-mail: rustem@icp.ac.ru*
[b]*Institut de Ciència de Materials de Barcelona (CSIC), Campus de la U. A. B., 08193 Bellaterra, Spain. E-mail: canadell@icmab.es; Fax: +34-93-5805729*
[c]*Lehrstuhl für Theoretische Chemie, Ruhr-Universität Bochum, 44780 Bochum, Germany*
[d]*Nijmegen High Field Magnet Laboratory, Toernooiveld 1, 6525 ED Nijmegen, The Netherlands*
[e]*International High Magnetic Fields and Low Temperatures Laboratory, 53-529 Wroclaw, Poland*

Received 8th October 2001, Accepted 15th November 2001
First published as an Advance Article on the web 15th January 2002

Tight-binding band structure calculations as well as magnetoresistance and magnetization measurements were carried out in order to characterize the Fermi surface of the novel organic metal $(BEDO\text{-}TTF)_5[CsHg(SCN)_4]_2$. The tight-binding calculations suggest that the Fermi surface can be described as containing two contributions: a closed two-dimensional portion associated with holes and an open pseudo-one-dimensional portion associated with electrons. Shubnikov-de Haas and de Haas-van Alphen oscillations were observed in magnetic fields of up to 14 T and temperatures of 1.5–4.2 K. Four frequencies ($F_1 = 650$ T, $F_2 = 2600$ T, $F_3 = 3200$ T and $F_4 = 3850$ T) associated with the Shubnikov-de Haas oscillations were found. The F_1 and F_4 frequencies are in good agreement with the calculated Fermi surface provided that the possibility of a magnetic breakdown effect is taken into account. It is also suggested that the F_2 and F_3 frequencies can be understood in the frame of the quantum interference effect.

Introduction

For a long time the series of organic conductors α-$(BEDT\text{-}TTF)_2MHg(SCN)_4$ (M = K,[1] Rb,[2] Tl[3] and NH_4,[4] BEDT-TTF: bis(ethylenedithio)tetrathiafulvalene) has attracted much attention due to the low-temperature phases with density-wave ordering and the intriguing magneto-oscillatory phenomena. Only one of the salts of this family is superconducting ($M = NH_4$ with $T_c \sim 1$ K)[5] and all others exhibit an antiferromagnetic phase transition at $T_p \sim (8–12)$ K where a shoulder-like resistance anomaly appears.[3,6–7] Below T_p these salts are characterized by anisotropic magnetic susceptibility[8] and a number of striking magnetoresistance anomalies.[9] All of these salts are isostructural and belong to the so-called α-phase family. Consequently, changing one of the anion partners in these three-component systems (M^+, $[Hg(SCN)_4]^{2-}$ and BEDT-TTF) does not influence the structure in a noticeable way but leads to a remarkable variety of physical behaviors.[10]

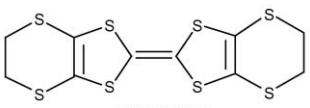

BEDT-TTF

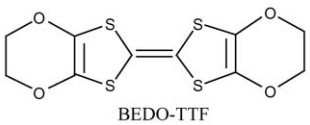

BEDO-TTF

In an attempt to further explore this type of material, we have recently synthesized new three-component systems based on the BEDO-TTF (bis(ethylenedioxy)tetrathiafulvalene) donor.[11] BEDO-TTF is an analogue of BEDT-TTF in which the four sulfur atoms of the peripheral rings have been changed to oxygen atoms.[12] Although BEDO-TTF is a chemical analogue of BEDT-TTF, it must be pointed out that BEDO-TTF itself is not isostructural with BEDT-TTF.[12,13] A large number of BEDO-TTF salts with different anions like I_3^-, IBr_2^-, $CF_3SO_3^-$, $Cu(SCN)_2^-$, *etc.* have been synthesized and structurally characterized.[14,15] The BEDO-TTF cation-radical salts are usually not isostructural with those of the BEDT-TTF donor and many of them adopt the so-called β″-type arrangement for their donor lattices.[16] Also in contrast with the large number of BEDT-TTF based superconductors is the fact that among the many BEDO-TTF based organic metals, only two of them have been found to be superconducting.[17,18]

Contrary to our expectations, the donor layers of the $(BEDO\text{-}TTF)_5[CsHg(SCN)_4]_2$ salt do not exhibit an α-type arrangement but, as most of the BEDO-TTF cation-radical salts, a β″-type one. In this work we would like to report a combined theoretical (tight-binding band structure calculations) and experimental (analysis of the observed Shubnikov-de Haas and de Haas-van Alphen oscillations) study in order to characterize the Fermi surface of $(BEDO\text{-}TTF)_5[CsHg(SCN)_4]_2$. Let us note that $(BEDO\text{-}TTF)_2ReO_4\cdot H_2O$,[18] which has been the focus of much attention because of its peculiar physical behaviour, possesses β″-type BEDO-TTF layers strongly related to those of the present salt, as well as a

similar average charge for the donors (0.4+ *vs.* 0.5+), and yet exhibits very different physical behaviour. It is hoped that our work will contribute to the detailed understanding of the correlation between the crystal structure, Fermi surface and electrical transport properties of the large class of BEDO-TTF salts with β″-type donor layers.

Experimental

Synthesis

Single crystals of $(BEDO\text{-}TTF)_5[CsHg(SCN)_4]_2$ were prepared[11] on a platinum anode by electrochemical oxidation of BEDO-TTF dissolved in 10% EtOH–1,2-dichloroethane or 10% EtOH–chlorobenzene at 0.3–0.9 μA cm^{-2} current density. $Hg(SCN)_2$ + CsSCN + crown ether or $Bu_4NHg(SCN)_3$ + CsSCN mixtures were used as supporting electrolytes.

Resistance and magnetoresistance

Resistance was measured using the standard dc four-probe method with 10 μm platinum wires and graphite paste, 10–100 μA current and temperatures down to 1.5 K. The Shubnikov-de Haas oscillations were observed by the ac (337 Hz) method with current (I = 100 μA) directed parallel to the c^*-axis. The de Haas-van Alphen oscillations were studied with a cantilever torquemeter.[19] The magnetic fields used were up to 14 T for both types of experiment and the temperature range was 1.5–4.2 K.

Band structure calculations

The tight-binding band structure calculations were based upon the effective one-electron Hamiltonian of the extended Hückel method.[20] The off-diagonal matrix elements of the Hamiltonian were calculated according to the modified Wolfsberg–Helmholz formula.[21] All valence electrons were explicitly taken into account in the calculations and the basis set consisted of double-ζ Slater-type orbitals for C, O and S, and single-ζ Slater-type orbitals for H. The exponents, contraction coefficients and atomic parameters for C, O, S and H were taken from previous work.[22]

Results and discussion

The crystal structure of $(BEDO\text{-}TTF)_5[CsHg(SCN)_4]_2$ (see Fig. 1a) is built from BEDO-TTF layers which alternate along the c-direction with inorganic layers wherein Cs^+ cations and $[Hg(SCN)_4]^{2-}$ anions form an extended two-dimensional network.[11] This structure differs from those of $(BEDT\text{-}TTF)_m[MHg(SCN)_4]$ salts with respect to both the donor and acceptor sublattices.[11] The donor layers in the present salt have a β″-type arrangement (see Fig. 1b) and are built from three different BEDO-TTF donors (A, B and C). There are three different types of intermolecular interactions within the slab of organic molecules, the relative orientation of which allows us to describe this layer as being composed of a series of parallel stacks of slipped donors along the (2*a*–*b*)-direction, as a series of step-chains along the (*a*+2*b*)-direction, or as a series of parallel chains of donors making lateral contacts along the (*a*–3*b*)-direction. The three types of chains have been labelled as 'slipped-chains', 'step-chains' and 'π-chains' in Fig. 1b.

The calculated band structure for the donor layers of $(BEDO\text{-}TTF)_5[CsHg(SCN)_4]_2$ near the Fermi level is reported in Fig. 2a. As shown in Fig. 1b, there are five donors per repeat unit of the layer so that the five bands of Fig. 2a are mainly built from the HOMO (highest occupied molecular orbital) of the BEDO-TTFs. The HOMOs of donors A, B and C are quite similar in energy (−8.43, −8.44 and –8.37 eV, respectively) so that they strongly mix and lead to the quite dispersive bands of

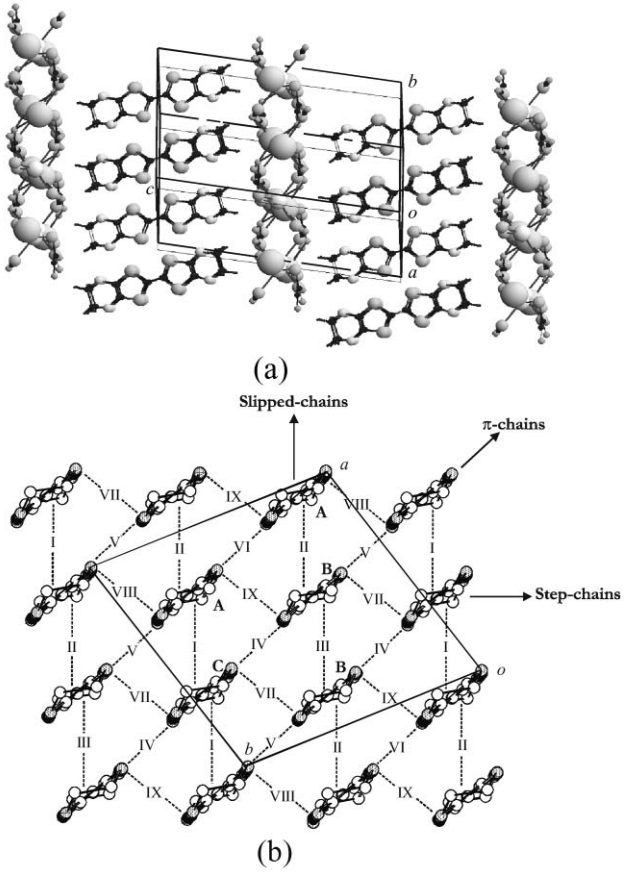

Fig. 1 (a) The crystal structure of $(BEDO\text{-}TTF)_5[CsHg(SCN)_4]_2$; (b) the donor layers of this salt where the different types of chains and donor···donor interactions have been labeled.

Fig. 2a. According to the usual oxidation states, the average charge of the donors is +0.4 and consequently, there should be two holes in the HOMO bands. In principle, the salt could

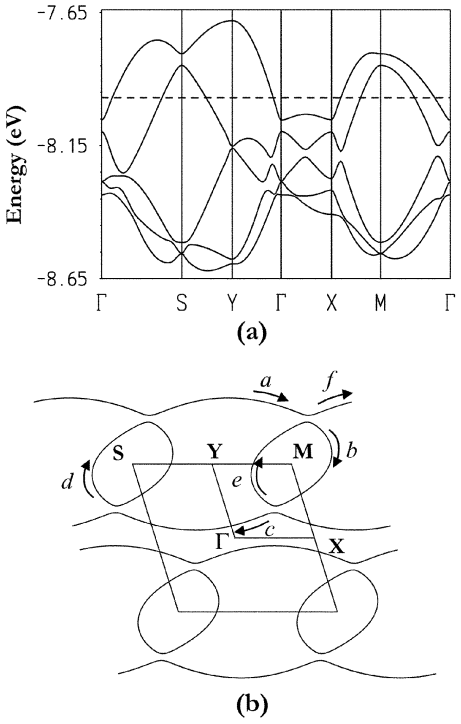

Fig. 2 Calculated (a) dispersion relations of the HOMO bands and (b) Fermi surface for the donor layers in $(BEDO\text{-}TTF)_5[CsHg(SCN)_4]_2$. The dashed line in (a) refers to the Fermi level and Γ = (0, 0), X = (a^*/2, 0), Y = (0, b^*/2), S = (−a^*/2, b^*/2) and M = (a^*/2, b^*/2).

be either a semiconductor (if there is a band gap between the two upper HOMO bands) or a metal (if the two upper bands overlap). As shown in Fig. 2a, the system is predicted to exhibit a metallic behaviour in agreement with the resistivity measurements (see below).

The Fermi surface associated with the band structure of Fig. 2a is shown in Fig. 2b. This Fermi surface can be described as having two contributions: a) a closed two-dimensional (2D) portion centred at M which is associated with holes, and b) an open pseudo-one-dimensional (pseudo-1D) portion which is warped and parallel to the a^*-direction, which is associated with electrons. However, the Fermi surface of Fig. 2b can be seen as a superposition of ellipses if we disregard the band hybridization, *i.e.*, the creation of gaps at the regions of interaction. This suggests that the system is a typical 2D metal despite the presence of open lines in the Fermi surface.

How the crystal and electronic structure of this material are related, as well as the relationship with other metallic BEDO-TTF salts with β″-donor layers, can be understood by looking at the different transfer integrals associated with the nine different pairs of HOMO···HOMO interactions in the donor layers (see Fig. 1b for the labelling of these interactions). The $t_{HOMO-HOMO}$ transfer integrals as well as the S···S contacts (note that the short S···O and O···O contacts do not influence the actual values of these integrals to any significant extent because the oxygen contribution to the HOMO of BEDO-TTF is very small[22]) associated with each type of donor···donor interaction are reported in Table 1. Note that the slipped-chains are associated with interactions I to III, the π-chains with interactions IV to VI and the step-chains with interactions VII to IX.

The important result in Table 1 is that the interactions along the step-chains and π-chains are comparable while those along the slipped-chains are considerably weaker (by a factor of two or three). That the interactions along the step-chains are among the strongest and that those along the slipped-chains are considerably smaller is hardly surprising in view of past experience with the analysis of the strength of the intermolecular interactions in many BEDT-TTF salts. Most surprisingly, and in stark contrast to the BEDT-TTF salts, the interactions along the π-chains, which result from a π-type overlap between the HOMOs, are comparable (if not even somewhat stronger) than those along the step-chains where the intermolecular overlap is of the more favourable σ-type. This is a result of the very short S···S intermolecular contacts within the π-chains (see Table 1) which override the intrinsic weakness of the π-type interactions with respect to the σ-type ones. These short contacts are a consequence of the smaller size of the oxygen atoms with respect to the sulfur ones, which allows for closer lateral contacts between the two almost coplanar donors.[14] This is an important difference from the β″-type BEDT-TTF layers which of course influences the shape of the respective Fermi surfaces.

Table 1 $t_{HOMO-HOMO}$ transfer integrals (meV) and S···S distances shorter than 4.0 Å[11] for the different donor···donor interactions in $(BEDO\text{-}TTF)_5[CsHg(SCN)_4]_2$.

Interaction type[a]	S···S distances/Å	$t_{HOMO-HOMO}$[b]/meV
I	3.659, 3.660	−62
II	3.661, 3.665	−43
III	3.671 (×2)	−38
IV	3.357, 3.402, 3.424	−147
V	3.317, 3.381, 3.431	−147
VI	3.347 (×2), 3.423	−149
VII	3.663, 3.681, 3.788	140
VIII	3.732, 3.738 (×2)	119
IX	3.710, 3.711, 3.776	126

[a]See Fig. 1b for labelling. [b]The transfer integrals have been calculated according to the usual dimer splitting approximation.[23]

Coming back to the fact that the interactions along the step-chains and π-chains are comparable while those along the slipped-chains are considerably weaker, let us note that this is the same situation as in the donor lattice of the 'parent' salt of this family, $(BEDO\text{-}TTF)_{2.4}I_3$[24] (*i.e.*, the repeat unit of the β″-type BEDO-TTF layers of this salt is just one donor). The $t_{HOMO-HOMO}$ transfer integrals along the slipped-chains, π-chains and step-chains of $(BEDO\text{-}TTF)_{2.4}I_3$ are −49, −142 and 146 meV, respectively. This means that, as far as the HOMO···HOMO interactions are concerned, the donor lattices of the two salts are very similar. Consequently, it should be possible to obtain the Fermi surface of $(BEDO\text{-}TTF)_5[CsHg(SCN)_4]_2$ by just appropriately folding the Fermi surface of the donor lattice of $(BEDO\text{-}TTF)_{2.4}I_3$, assuming the same average charge (*i.e.*, +0.4) for the donor. $(BEDO\text{-}TTF)_{2.4}I_3$ exhibits a typical Fermi surface for a two-dimensional metal:[14] a closed loop with elliptical shape centred at the ($b^*/2$, 0) point of the 2D Brillouin zone (b is the repeat vector along the slipped-stacks of this salt[24]). This shape is kept for a BEDO-TTF average charge of +0.4 (*i.e.*, the appropriate average charge for $(BEDO\text{-}TTF)_5[CsHg(SCN)_4]_2$). The repeat unit for the donor layers of $(BEDO\text{-}TTF)_5[CsHg(SCN)_4]_2$ contains five donors (see Fig. 1b). Thus the repeat unit is five times larger than that of the parent layers of $(BEDO\text{-}TTF)_{2.4}I_3$ and, consequently, the Brillouin zone for our 2D calculation should be five times smaller. This means that the Fermi surface for the donor layers of the present salt must be the appropriately folded version (care must be taken of the fact that the two repeat vectors are directed along different directions in the two salts) of the ellipse-shape Fermi surface of $(BEDO\text{-}TTF)_{2.4}I_3$ assuming a +0.4 charge for the donors. The expected Fermi surface on the basis of this reasoning is exactly that of Fig. 2b in which the weakly avoided crossings become real crossings. Because of the weakly avoided crossings (a consequence of the fact that the three different transfer integrals associated with a given type of chain are not identical), there is a formally closed portion centred at M and a pair of wavy lines parallel to the a^*-direction in the real Fermi surface. This Fermi surface has no nesting properties and consequently, it is not expected that $(BEDO\text{-}TTF)_5[CsHg(SCN)_4]_2$ can exhibit density wave type instabilities leading to the total or partial suppression of the metallic state.

On the basis of the Fermi surface of Fig. 2b, it is predicted that at least one Shubnikov-de Haas frequency corresponding to an approximate (remember that the calculations have been carried out using the room temperature structure) cross sectional area of 19% of the first Brillouin zone should be observable in the magnetoresistance experiments. In view of the weakly avoided crossings in Fig. 2b, a second frequency corresponding to the full ellipse (*i.e.*, due to the magnetic breakdown effect) should also be observable. Since the magnetic breakdown orbit corresponds to the ellipse of the unfolded Fermi surface and given the average charge of the donor (+0.4 which corresponds to one-fifth of the 2D unfolded first Brillouin zone) this frequency should correspond to a cross sectional area of 100% of the first Brillouin zone.

The temperature dependence of the resistance of the quasi-2D metal $(BEDO\text{-}TTF)_5[CsHg(SCN)_4]_2$ was measured with current parallel ($\rho_{\|}$) (Fig. 3) and perpendicular ($\rho_{\perp}$) (inset in Fig. 3) to the conducting plane of the crystal. As can be seen in Fig. 3 $\rho_{\|}$ exhibits a 'hump' at about 50 K. Let us remark that it is possible to find crystals in the same batch which exhibit a very small 'hump' or even crystals in which this hump can not be seen at all. This is connected with the quality of the crystals. Microprobe analysis of the different crystals led to the same results. The increase in resistance with temperature and the 'hump' in $\rho_{\|}$ are not connected with a phase transition. The excellent agreement between the Fermi surface parameters calculated from X-ray data at room temperature and the quantum oscillations results obtained at helium temperatures

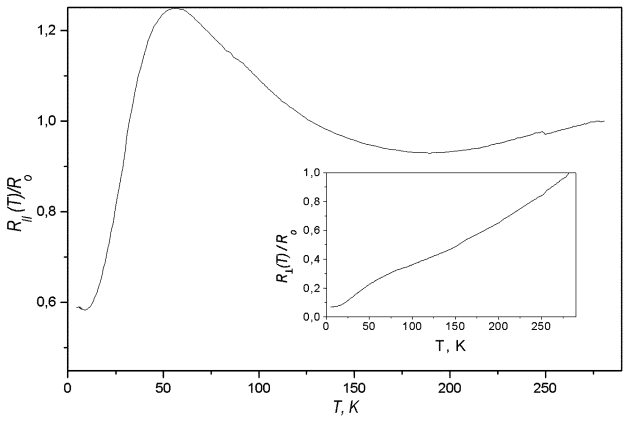

Fig. 3 Temperature dependence of the resistance for current parallel to the conducting plane (see inset for current perpendicular to the conducting plane)

(see below) support this conclusion. The resistance anisotropy $\rho_{\perp}/\rho_{\parallel}$ is approximately 10^4 at room temperature and changes considerably when temperature decreases.

Shubnikov–de Haas (SdH) and de Haas–van Alphen (dHvA) quantum oscillations were observed in crystals studied at different magnetic field directions and temperatures. Fig. 4 shows an example of these SdH oscillations. It should be noted that no beating node occurs in these oscillations, suggesting again a strong 2D electronic character with a negligible warping of the Fermi surface. The spectrum of these oscillations contains four frequencies: $F_1 \approx 650$ T, $F_2 \approx 2600$ T, $F_3 \approx 3200$ T, $F_4 \approx 3850$ T for the field direction perpendicular to the conducting plane (Fig. 5). The dependence of these frequencies on the angle between the field direction and the direction perpendicular to the conducting plane can be described by the relation $F_i(\theta) = F_i(0)/\cos\theta$, which is the expected one for quasi-2D Fermi surface sections (*i.e.*, cylinder-like Fermi surfaces). The frequency F_1 corresponds to a cross sectional area of 16% of the first Brillouin zone and originates from the closed part of the Fermi surface (see Fig. 2b). The frequency F_4 corresponds to an area of 100% of the first Brillouin zone and most likely results from a magnetic breakdown orbit including parts of the closed and open portions of the Fermi surface (see Fig. 2b). Consequently, the F_1 and F_4 frequencies are in good agreement with the results of our theoretical study. Two additional frequencies, $F_2 \approx F_4 - 2F_1$ and $F_3 \approx F_4 - F_1$, correspond to the forbidden orbits. From a quantum-mechanical point of view there is no semiclassical closed orbit to explain these frequencies. However, they can be understood in the frame of the quantum

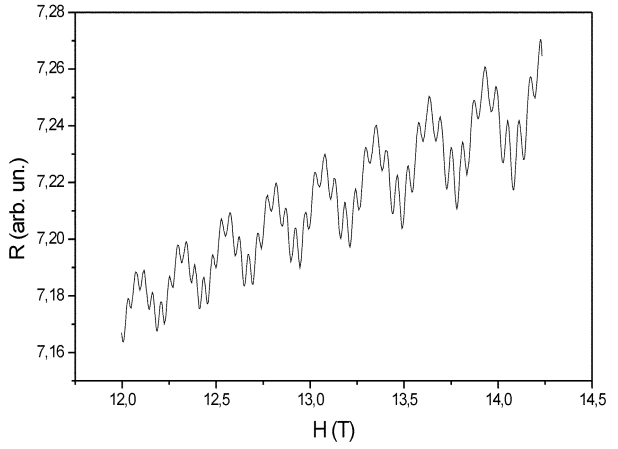

Fig. 4 Shubnikov-de Haas oscillations in the organic metal (BEDO-TTF)$_5$[CsHg(SCN)$_4$]$_2$ for the field direction parallel to the c^*-axis ($\theta = 0^\circ$) and $T = 1.55$ K.

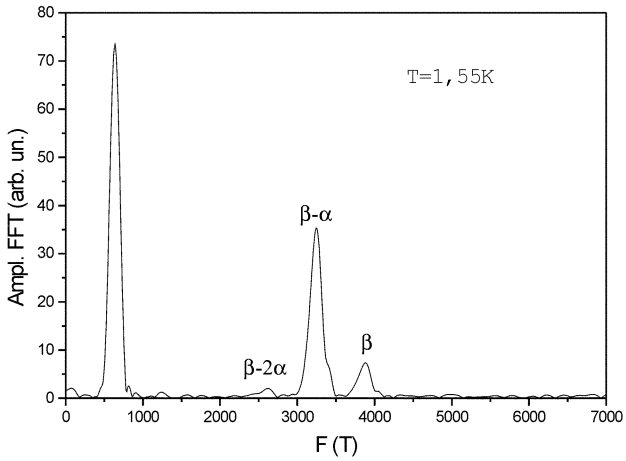

Fig. 5 Fast Fourier transform spectrum of the oscillations from Fig. 4. Four different frequencies $F_1 \sim 650$ T, $F_2 \sim 2600$ T, $F_3 \sim 3200$ T and $F_4 \sim 3850$ T are clearly seen.

interference (QI) model[25] as two-arms Stark interferometers.[26] Within the QI model[25] the temperature damping of the oscillation amplitude is given by the energy derivative of the phase difference $(\varphi_i - \varphi_j)$ between two different routes i and j of a two-arms interferometer. This model states that $\partial(\varphi_i - \varphi_j)/\partial\varepsilon = (\hbar eB)\ \partial S_k/\partial\varepsilon$, where S_k is the reciprocal space area bounded between two arms. Since $\partial(\varphi_i - \varphi_j)/\partial\varepsilon$ is proportional to the difference between the effective masses of the two arms of the interferometer, the associated effective mass is given by $m^* = |m_i^* - m_j^*|$, where m_i^* and m_j^* are the partial effective masses of the routes i and j. In our case an interferometer connected with the frequency F_3 consists of two routes, *abcdaf* and *abef*, and another interferometer, connected with the frequency F_2, includes two cyclotron orbits, *abcdaf* and *abebef* (see Fig 2b).

According to Falicov and Stahowiak[27] the contribution of every segment of the cyclotron orbit to the cyclotron mass parameter is proportional to the subtended angle of this segment, and the total cyclotron mass parameter equals the sum of the partial cyclotron mass parameters. We have estimated the effective mass parameters from the temperature dependence of the SdH oscillation amplitude using the standard formula $R_T \sim rz/\sin h\ (rz)$, with $z = \alpha m^* T/B$ where $\alpha = 14.69\ \mathrm{T\,K^{-1}}$ and m^* is the cyclotron effective mass (relative to the free electron mass m_e). The field window 12–14 T and temperature range 1.5–4.2 K were used for the fast Fourier transform (FFT) analysis of the amplitudes. We have obtained the following values for the effective mass parameters: $m_1 = (1.6 \pm 0.1)m_e$, $m_2 = (0 \pm 0.3)m_e$, $m_3 = (1.5 \pm 0.1)m_e$ and $m_4 = (3.0 \pm 0.3)m_e$. This estimation shows that $m_3 \sim m_4 - m_1 = m_{abcdaf} - m_{abef}$ and $m_2 \sim m_4 - 2m_1 = m_{abcdaf} - m_{abebef}$, where m_{abcdaf}, m_{abef} and m_{abebef} are the partial effective masses of the routes *abcdaf*, *abef* and *abebef*, respectively.

It is interesting to compare the temperature dependence of the amplitude for all frequencies (see Fig. 5 for $T = 1.55$ K and Fig. 6 for $T = 4.2$ K). At 1.55 K the α and (β–α) oscillation amplitudes dominate whereas the (β–2α) amplitude oscillation is very small. However, the (β–2α) amplitude oscillation dominates and the β one disappears completely at 4.2 K. These results are in agreement with the effective mass values corresponding to these oscillation frequencies and satisfy the necessary relations between effective masses for the QI effect. Noting that below 4.2 K the oscillation amplitude connected with the (β–2α) frequency is constant within experimental error (*i.e.*, a zero cyclotron mass), we may assume that this oscillation can survive to considerably higher temperatures. An analogous situation has been previously found for the κ-(BEDT-TTF)$_2$Cu(NCS)$_2$ salt.[28]

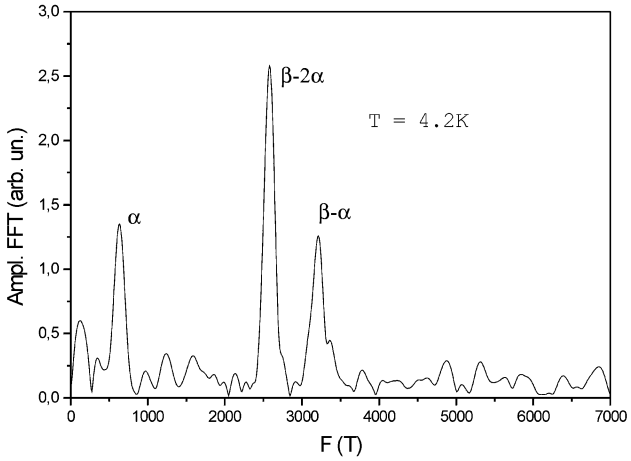

Fig. 6 Fast Fourier transform spectrum of the Shubnikov-de Haas oscillations at 4.2 K for an angle $\theta = 0°$. The frequency F_4 is absent and the frequency F_2 dominates.

It is well known[29–31] that the Stark QI effect should not contribute to the free energy and does not manifest itself in the thermodynamic properties of the system, so it can not contribute to the magnetic oscillations giving rise to the de Haas-van Alphen effect. Fig. 7 shows the dHvA oscillations for the present salt at 1.55 K and the FFT is shown in Fig. 8. Only two frequencies, α and β, can be seen so this can be taken

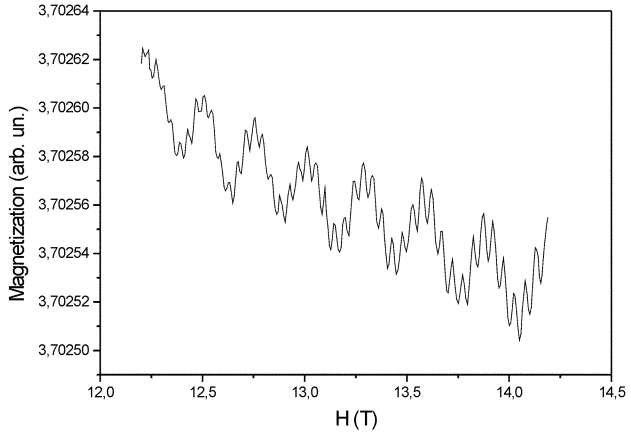

Fig. 7 De Haas-van Alphen oscillations in $(BEDO\text{-}TTF)_5[CsHg(SCN)_4]_2$ at 1.55 K for an angle $\theta = 14°$.

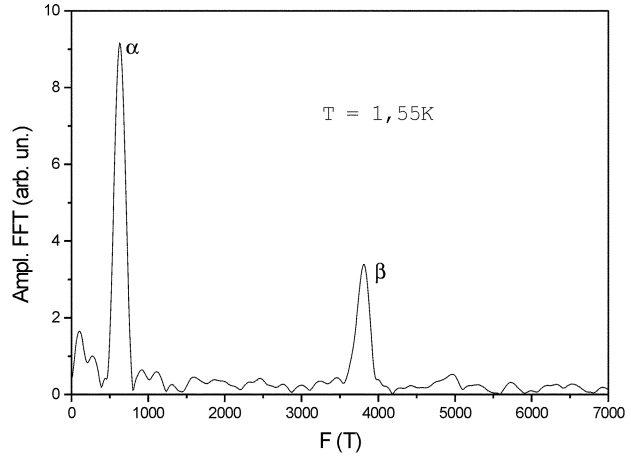

Fig. 8 Fast Fourier transform spectrum of the oscillations from Fig. 7. Only the two frequencies F_1 and F_4 are observed.

as additional confirmation of the fact that the (β–α) and (β–2α) frequencies are really connected with a QI effect.

In conclusion, the behaviour of the quantum oscillations in $(BEDO\text{-}TTF)_5[CsHg(SCN)_4]_2$ seems to be in good agreement with the predictions of the tight-binding band structure calculations. The additional frequencies in the SdH oscillation spectrum are most probably caused by the quantum interference effect. Thus, we propose that Fig. 2b provides an adequate description of the Fermi surface of $(BEDO\text{-}TTF)_5[CsHg(SCN)_4]_2$ and that the frequencies (β–α) and (β–2α) are connected with magnetic breakdown and the QI effect.

Acknowledgement

This work was supported by RFBR 01-03-33009, NWO-grant 4359, DGI-Spain (Project BFM2000-1312-C02-01) and Generalitat de Catalunya (Project 1999 SGR 207).

References

1 M. Oshima, H. Mori, G. Saito and K. Oshima, *Chem. Lett.*, 1989, 1159.
2 H. Mori, S. Tanaka, K. Oshima, M. Oshima and G. Saito, *Solid State Commun.*, 1990, **74**, 1261.
3 D. Kushch, L. I. Buravov, M. V. Kartsovnik, V. N. Laukhin, S. I. Pesotskii, R. P. Shibaeva, L. P. Rosenberg, E. B. Yagubskii and A. V. Zvarykina, *Synth. Met.*, 1992, **46**, 271.
4 H. Mori, S. Tanaka, M. Oshima, G. Saito, T. Mori, Y. Maruyama and H. Inokuchi, *Bull. Chem. Soc. Jpn*, 1990, **63**, 2183.
5 H. H. Wang, K. D. Karlson, U. Geiser, W. K. Kwok, M. D. Vashon, I. E. Tompson, N. F. Larsen, G. D. McCaba, R. S. Holcherand and J. M. Williams, *Physica C (Amsterdam)*, 1990, **166**, 57.
6 N. Kinoshita, M. Tokumoto and H. Anzai, *J. Phys. Soc. Jpn.*, 1991, **60**, 2131.
7 T. Sasaki, N. Toyota, M. Tokumoto, N. Kinoshita and H. Anzai, *Solid State Commun.*, 1990, **75**, 93.
8 T. Sasaki, H. Sato and N. Toyota, *Synth. Met.*, 1991, **41-43**, 2211.
9 J. Caulfield, S. J. Blundell, M. S. L. du Croo de Jongh, P. T. Hendriks, J. Singleton, M. Doporto, F. L. Pratt, A. House, J. A. A. J. Perenboom, W. Hayes, M. Kurmoo and P. Day, *Phys. Rev. B*, 1995, **51**, 8325.
10 See for instance: *Proc. Int. Conf. on the Science and Technology of Synthetic Metals* (Snowbird, UT, 1996); *Synth. Met.*, 1997, **85** + **86**.
11 E. I. Zhilyaeva, O. A. Bogdanova, R. N. Lyubovskaya, R. B. Lyubovskii, K. A. Lyssenko and M. Yu. Antipin, *Synth. Met.*, 1999, **99**, 169.
12 T. Suzuki, H. Yamochi, G. Srdanov, K. Hincelman and F. Wudl, *J. Am. Chem. Soc.*, 1989, **111**, 3108.
13 H. Kobayashi, A. Kobayashi, Y. Sasaki, G. Saito and H. Inokuchi, *Bull. Chem. Soc. Jpn.*, 1986, **59**, 301.
14 S. Horiuchi, H. Yamochi, G. Saito, K. Sakaguchi and M. Kusunori, *J. Am. Chem. Soc.*, 1996, **118**, 8604.
15 L. V. Zorina, S. S. Khasanov, R. P. Shibaeva, M. Gener, R. Rousseau, E. Canadell, L. A. Kushch, E. B. Yagubskii, O. O. Drozdova and K. Yakushi, *J. Mater. Chem.*, 2000, **10**, 2017.
16 (*a*) T. Mori, *Bull. Chem. Soc. Jpn.*, 1998, **71**, 2509; (*b*) T. Mori, H. Mori and S. Tanaka, *Bull. Chem. Soc. Jpn.*, 1999, **72**, 179.
17 M. A. Beno, H. H. Wang, A. M. Kini, K. D. Karlson, U. Geiser, W. K. Kwok, J. E. Tompson and J. M. Williams, *Inorg. Chem.*, 1990, **29**, 1599.
18 S. Kahlich, D. Schweitzer, J. Heinen, S. E. Lan, B. Nuber, H. J. Keller, K. Winzer and H. W. Helberg, *Solid State Commun.*, 1991, **8**, 191; L. I. Buravov, A. G. Khomenko, N. D. Kushch, V. N. Laukhin, A. I. Schegolev, E. B. Yagubskii, L. P. Rozenberg and R. P. Shibaeva, *J. Phys. I France*, 1992, **2**, 529.
19 P. Christ, W. Biberacher, H. Muller and K. Andres, *Solid State Commun.*, 1994, **91**, 451.
20 M.-H. Whangbo and R. Hoffmann, *J. Am. Chem. Soc.*, 1978, **100**, 6093.
21 J. Ammeter, H.-B. Bürgi, J. Thibeault and R. Hoffmann, *J. Am. Chem. Soc.*, 1978, **100**, 3686.
22 S. S. Khasanov, B. Zh. Narymbetov, L. V. Zorina, L. P. Rosenberg, R. P. Shibaeva, N. D. Kushch, E. B. Yagubskii, R. Rousseau and E. Canadell, *Eur. Phys. J. B*, 1988, **1**, 419.
23 P. M. Grant, *J. Phys. (Paris)*, 1983, **44**, C3–847.
24 F. Wudl, H. Yamochi, T. Suzuki, H. Isotalo, C. Fite, H. Kasmai,

K. Liou, G. Srdanow, P. Coppens, K. Maly and A. Frost-Jensen, *J. Am. Chem. Soc.*, 1990, **112**, 2461.
25 R. W. Stark and C. B. Freiberg, *J. Low Temp. Phys.*, 1974, **14**, 111.
26 D. Shoenberg, *Magnetic Oscillations in Metals*, Cambridge University Press, Cambridge, UK, 1984.
27 L. M. Falicov and H. Stahowiak, *Phys. Rev.*, 1966, **147**, 505.
28 M. V. Kartsovnik, G. Yu. Logvenov, T. Ishiguro, W. Biberacher, H. Anzai and N. D. Kushch, *Phys. Rev. Lett.*, 1996, **77**, 2530.
29 R. W. Stark and R. Reifenberger, *J. Low Temp. Phys.*, 1977, **26**, 763.
30 D. Morosin and R. W. Stark, *J. Low Temp. Phys*, 1981, **45**, 531.
31 M. I. Kaganov and A. A. Slutskin, *Phys. Rep.*, 1983, **98**, 189.